

The influence of collective behavior on the magnetic and heating properties of iron oxide nanoparticles

C. L. Dennis,^{1,a)} A. J. Jackson,^{2,3} J. A. Borchers,² R. Ivkov,⁴ A. R. Foreman,⁴ J. W. Lau,¹ E. Goernitz,⁵ and C. Gruettner⁶

¹Materials Science and Engineering Laboratory, NIST, Gaithersburg, Maryland 20899-8552, USA

²NIST Center for Neutron Research, Gaithersburg, Maryland 20899-8562, USA

³Department of Materials Science and Engineering, University of Maryland, College Park, Maryland 20742, USA

⁴Triton BioSystems, Inc., Chelmsford, Massachusetts 01824, USA

⁵Fraunhofer Institut Angewandte Polymerforschung, 14476 Potsdam-Golm, Germany

⁶Micromod Partikeltechnologie GmbH, 18119 Rostock-Warnemuende, Germany

(Presented on 6 November 2007; received 11 September 2007; accepted 15 November 2007; published online 26 March 2008)

Magnetic nanoparticles with a high specific absorption rate (SAR) have been developed and used in mouse models of cancer. The magnetic nanoparticles are comprised of predominantly iron oxide magnetic cores surrounded by a dextran layer for colloidal stability. The average diameter of a single particle (core plus dextran) is 92 ± 14 nm as measured by photon correlation spectroscopy. Small angle neutron scattering measurements under several H₂O/D₂O contrast conditions and at varying nanoparticle concentrations have revealed three length scales: $>10 \mu\text{m}$, several hundred nanometers, and tens of nanometers. The latter corresponds to the particle diameter; the several hundred nanometers corresponds to a hard sphere interaction radius of the core/shell nanoparticles; $>10 \mu\text{m}$ corresponds to the formation of long-range, many-particle structures held together by magnetic interactions and dextran. The long-range collective magnetic behavior appears to play a major role in enhancing the SAR. For samples having nominally equal concentrations and similar saturation magnetizations, the measured SAR is 1075 W/(g of Fe) for tightly associated nanoparticles and 150 W/(g of Fe) for very loosely associated nanoparticles at an applied field of 86 kA/m (1080 Oe) and 150 kHz. © 2008 American Institute of Physics.

[DOI: [10.1063/1.2837647](https://doi.org/10.1063/1.2837647)]

INTRODUCTION

The biological processes in cells, including cancer, are particularly susceptible to changes in temperature. In fact, a change in temperature of 6 °C, from 37 to 43 °C, is sufficient to kill a cancer cell provided the cell is exposed to this temperature for a sufficient period of time.^{1,2} While the biology of thermal damage is well understood, this knowledge has translated poorly into clinical application for cancer therapy, although some success has been achieved for classic hyperthermia^{3,4} treatment. One reason is the absence of technology that effectively localizes heat to the tumor without heating surrounding healthy tissues.⁵ A second limitation is the inability to accurately measure the heat dose deposited into the tumor relative to surrounding tissue.^{6,7} One technology being developed to address these limitations is the activation of susceptor materials such as magnetic iron oxide nanoparticles by excitation with an external alternating magnetic field. However, the lack of information on which characteristics are important for delivering the maximum heat dose per gram of injected material^{8,9} is a significant issue. It is the objective of this paper to address this issue; in particular, to identify one characteristic that is important for delivering the maximum heat dose per gram of injected material.

EXPERIMENTAL METHODS

The system studied here is based on iron oxide magnetic cores that are coated with dextran to form a shell, and have a diameter less than 50 nm. The samples were synthesized by high-pressure homogenization according to the core/shell method, as outlined previously.¹⁰ Two different sample batches were studied here. Although these two systems are nominally identical in their cores, the dextran layer itself varies: Lot 0020784G (20784G) was coated with dextran once yielding a single dextran layer while Lot 01350684G (50684G) was coated twice for a double dextran layer.

A variety of analytical techniques have been applied to physically characterize these two systems. Analytical ultracentrifugation (AUC) was used to determine a density for the nanoparticles and an accurate size and size distribution for the iron oxide core. Photon correlation spectroscopy (PCS) was used to determine an average size and size distribution of the entire core/shell structure. The hysteresis loops were measured with a superconducting quantum interference device (SQUID) magnetometer from Quantum Design.¹¹ All of the measurements were made at room temperature (298 K) using a Kel-F liquid capsule holder from LakeShore Cryotronics¹¹ to hold the colloid, and the field range was from ± 3.98 MA/m (± 50 000 Oe).

The small angle neutron scattering (SANS) experiments were conducted at the NG-3 beam line at the NIST Center for Neutron Research (NCNR) using neutrons with a wave-

^{a)}Electronic mail: cindi.dennis@nist.gov.

length of 8.4 Å. Data were collected with a two-dimensional detector at three different sample-to-detector distances, in order to span the range of scattering vectors Q from 7×10^{-4} to 5×10^{-1} Å⁻¹. The data were corrected for instrumental and empty cell backgrounds. To probe smaller Q values, ultra-SANS (USANS) experiments were performed using the BT5 thermal neutron double-crystal instrument at NCNR.¹² The samples were run for 8 h each at a neutron wavelength of 2.4 Å. A background from an empty beam run was subtracted from all the data, and the subtracted data processed to absolute scale. The Q (wave vector component in the horizontal plane) range corresponds to probing length scales from 500 to 20 000 nm. All of the SANS and USANS measurements were made at room temperature and in zero field. A series of concentrations were also used in order to help constrain the parameters for the fitting. All SANS and USANS reductions and fits were performed by the use of interactive IGOR¹¹ procedures.¹³

Specific absorption rate (SAR) measurements, to determine the heat dose of the nanoparticles, were made in a modified alternating magnetic field (AMF) calorimeter under varying field amplitudes at a frequency of 150 kHz. SAR values were calculated from the rate of temperature rise measured in the water when the particle suspension was heated by the AMF generated in a solenoid coil, after correction for the thermal properties of the calorimeter, coil, and water. The values were normalized for iron content.

RESULTS AND DISCUSSION

AUC yielded a density of 3.20 g/cm³, which is slightly less than that of bulk iron oxide at 5.18 g/cm³, and a size distribution of 44 ± 13 nm for the nanoparticle core. PCS yielded a larger size and size distribution of 92 ± 14 nm. This number is the same whether it is determined by intensity or by volume. However, the PCS instrument estimates a hydrodynamic radius based on a Stokes–Einstein sphere moving through the solvent and thus includes an estimate of the thickness of the dextran layer infiltrated with solvent. A dextran length of 24 nm is reasonable for the 40 000 Da dextran used. The AUC data also agree with the TEM images (not shown) that show a core diameter of ~ 50 nm. The dextran layer thickness cannot be determined from the TEM as (a) it is a dried sample and (b) it is difficult to separate the amorphous dextran from the amorphous carbon film coating the TEM grid at this excitation energy.

The SANS/USANS data are also in reasonable agreement with these numbers. The 50684G data, both H₂O and D₂O, are shown in Fig. 1. (The concentration series is not shown for space reasons.) H₂O and D₂O each highlight different features of the system by varying the sample contrast. In the case of H₂O the scattering is dominated by the large contrast between iron oxide and H₂O, whereas there is less contrast with dextran. In D₂O the intensity of scattering from the core is much reduced while the contrast with dextran is enhanced. The 50684G in D₂O data show a strong scattering intensity at low Q that may be due to the presence of a dextran network acting to bind particles in large scale aggregates.¹⁴ This interpretation agrees with other observa-

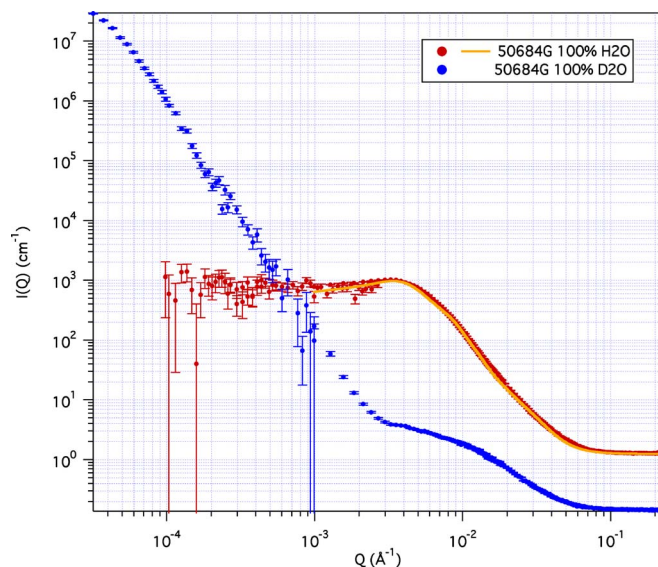


FIG. 1. (Color online) SANS/USANS data and fits on the 50684G samples in two contrasts. The D₂O data highlight both the iron oxide core (the “hump” around $Q=4 \times 10^{-2}$) and the dextran (the slope for $Q < 1 \times 10^{-3}$). The H₂O data highlight just the iron oxide core.

tions of dextran solutions.¹⁵ A polydispersed core-shell model was used to fit the H₂O data by keeping the ratio of core to shell sizes constant. The hard sphere interaction radius is determined to be 69.5 ± 0.2 nm, indicating that there is an interaction on a length scale longer than the particle size visible to neutrons.

The SANS data from the 20784G sample are shown in Fig. 2. The concentration series in H₂O is shown, while the D₂O data that are similar to those in Fig. 1 are excluded. Here the interaction radius is >200 nm—a factor of 3 larger than for the 50684G sample. It should be noted that this increase in the interaction radius is not due to a change in average diameter (as determined earlier by both AUC and PCS), nor by a change in volume fraction. From SANS/

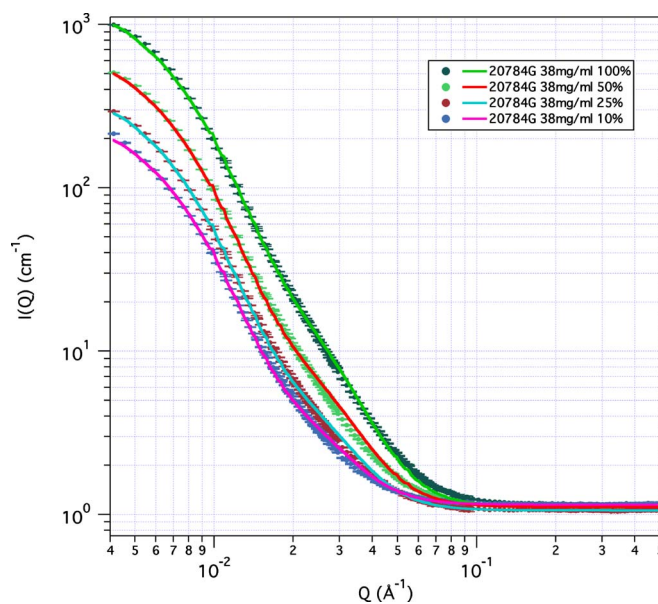


FIG. 2. (Color online) SANS data and fits on the 20784G samples in a concentration series H₂O. The iron oxide core structure is in the hump.

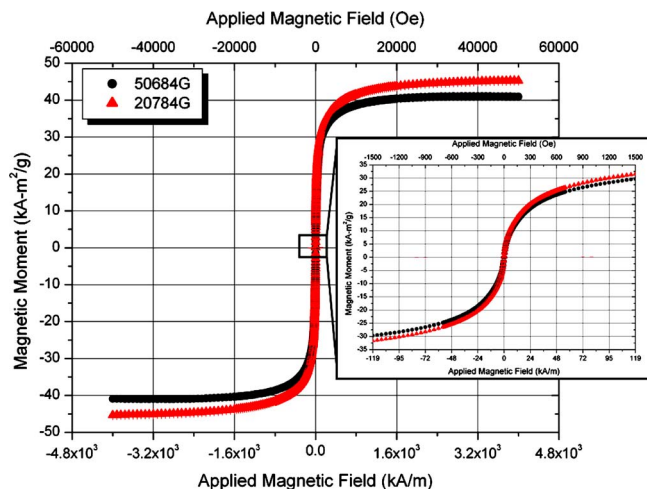


FIG. 3. (Color online) Hysteresis Loop at 298 K of the 50684G and 20784G samples, normalized to mass of iron oxide. The inset shows a closeup of the data around the two fields of interest—0 and 86 kA/m (1080 Oe).

USANS, the volume fractions of both samples are nearly equal (0.1075 ± 0.0005 for 50684G and 0.1050 ± 0.0003 for the 20784G sample), as is the polydispersity—an indicator of the size distribution—which is 0.6.

The magnetic properties of the system were characterized by measuring the hysteresis loop at room temperature. These loops (see Fig. 3) have been normalized to the mass of particles present in the colloid. The most prominent point is that the saturation magnetization of the 50684G sample is 41.08 ± 0.03 kA m²/g, slightly less than that of the 20784G sample which is 45.34 ± 0.02 kA m²/g. Other than this slight difference in magnitude, the shapes of the two hysteresis loops are nearly identical. It is noteworthy that the SANS data exhibit significantly different interaction radii in zero field for the two samples, although the SQUID data show nearly identical magnetic moments at the fields used in the SAR measurements.

The SAR values were measured for $H=86$ kA/m (1080 Oe) and $f=150$ kHz using colloids of nominally equal concentrations which are then normalized to iron concentration. Here we see the most striking difference—the 50684G sample has a measured SAR of 1075 W/(g of Fe) while the 20784G has a measured SAR of 150 W/(g of Fe)—a difference of a factor of 7. This cannot be attributed to a difference in the saturation magnetizations as these are shown, first, to have the opposite trend, and second, to differ only by 10%. Nor can this be attributed to differences in the physical size or size distribution as these have been shown through three physical techniques (TEM, AUC, and PCS) to be nearly the same. However, the primary difference appears in the SANS/USANS data in the interaction behavior. The double dextran layer has a much smaller interaction radius, by nearly a factor of 3. This smaller interaction radius would have a twofold effect: (1) the dipolar interactions would be significantly stronger, enabling the nanoparticles to couple their behavior under an oscillating field (thereby amplifying the heating) and (2) the smaller interaction radius would mean that more particles are grouped closer together, enhancing the local heat output in a smaller area. This latter effect is expected to

show significant enhancement in the efficacy of these particles in preclinical trials. Model simulations and ac measurements in conjunction with mouse trials are underway to confirm these effects.

CONCLUSIONS

Although the magnetic properties of a sample (saturation magnetization, anisotropy, and volume) are expected to have significant effects on the heat dose supplied by magnetic nanoparticles under the influence of an alternating magnetic field, the individual nanoparticle properties are not the only consideration. The behavior of the collection of magnetic nanoparticles is equally critical in determining the heat dose, as demonstrated by two nominally identical systems of 44 nm iron oxide core/shell nanoparticles. The tightly associated system has a measured SAR of 1075 W/(g of Fe), while the more loosely associated system has a SAR of 150 W/(g of Fe). This is expected to have significant effects in the efficacy of the nanoparticles for cancer treatment.

ACKNOWLEDGMENTS

This work is supported by the U.S. Army Medical Research and Materiel Command under Contract No. W81XWH-04-C-0142. The views, opinions, and/or findings contained in the report are those of the author(s) and should not be construed as an official Department of the Army position, policy, or decision unless so designated by other documentation. This work utilized facilities supported in part by the National Science Foundation under Agreement No. DMR-0454672.

¹J. Overgaard, in *Hyperthermic Oncology*, edited by J. Overgaard (Taylor and Francis, London, 1985), Vol. 2, pp. 8–9.

²C. Steffler and D. van Beuningen, in *Hyperthermia and the Therapy of Malignant Tumors*, edited by J. Steffler (Springer, Berlin, 1987), pp. 24–70.

³N. Zaffaroni, G. Fliorentini, and U. De Giorgi, *Eur. J. Surg. Oncol.* **27**, 340 (2001).

⁴P. Moroz, S. K. Jones, and B. N. Gray, *J. Surg. Oncol.* **80**, 149 (2002).

⁵S. J. DeNardo, G. L. DeNardo, A. Natarajan, L. A. Miers, A. R. Foreman, C. Gruettner, G. N. Adamson, and R. Ivkov, *J. Nucl. Med.* **48**, 437 (2007).

⁶M. W. Dewhirst, E. Jones, T. Vujaskovic, C. Li, and L. Prosnitz, in *Cancer Medicine*, edited by D. Kufe, R. Pollock, R. Weichselbaum, R. Bast, Jr., and T. Gansler (Hamilton, Ontario, 2003), pp. 623–636.

⁷J. van der Zee, *Ann. Oncol.* **13**, 1173 (2002).

⁸S. J. DeNardo, G. L. DeNardo, L. A. Miers, A. Natarajan, A. R. Foreman, C. Gruettner, G. N. Adamson, and R. Ivkov, *Clin. Cancer Res.* **11**, 7087s (2005).

⁹P. J. Hoopes, R. Strawbridge, U. J. Gibson, Q. Zeng, Z. Pierce, M. Saveliano, J. A. Tate, J. A. Ogden, I. Baker, R. Ivkov, A. R. Foreman, C. Gaito, L. Dulatas, J. Tate, and J. Ogden, *Proc. SPIE* **6440**, 6440K (2007).

¹⁰C. Gruettner, K. Mueller, J. Teller, F. Westphal, A. Foreman, and R. Ivkov, *J. Magn. Magn. Mater.* **311**, 181 (2007).

¹¹The identification of any commercial product or trade name does not imply endorsement or recommendation by NIST.

¹²J. G. Barker, C. J. Glinka, J. J. Moyer, M. H. Kim, A. R. Drews, and M. Agamalian, *J. Appl. Crystallogr.* **38**, 1004 (2005).

¹³S. R. Kline, *J. Appl. Crystallogr.* **39**, 895 (2006).

¹⁴The extended length scales observed in SANS/USANS are not seen in the PCS data because the sample concentration in the PCS sample and the SANS/USANS/SAR sample differ by about two orders of magnitude (0.12 mg Fe/ml versus ~ 13.4 mg Fe/ml) due to practical measurement considerations.

¹⁵C. Galant, C. Amiel, V. Wintgens, and B. Seville, *Langmuir* **18**, 9687 (2002).